9-1-2007

Snell's Law of Refraction Observed in Thermal Frontal Polymerization

John A. Pojman
University of Southern Mississippi

Veronika Viner
University of Southern Mississippi

Burcu Binici
University of Southern Mississippi

Shanna Lavergne
University of Southern Mississippi

Melanie Winsper
University of Southern Mississippi

See next page for additional authors

Snell's law of refraction observed in thermal frontal polymerization

John A. Pojman, Veronika Viner, Burcu Binici, Shanna Lavergne, and Melanie Winsper
Department of Chemistry and Biochemistry, The University of Southern Mississippi, Hattiesburg, Mississippi 39406, USA

Dmitry Golovaty and Laura Gross
Department of Theoretical and Applied Mathematics, The University of Akron, Akron, Ohio 44325-4002, USA

(Received 30 May 2007; accepted 22 August 2007; published online 28 September 2007)

We demonstrate that Snell's law of refraction can be applied to thermal fronts propagating through a boundary between regions that support distinct frontal velocities. We use the free-radical frontal polymerization of a triacrylate with clay filler that allows for two domains containing two different concentrations of a peroxide initiator to be molded together. Because the polymerization reaction rates depend on the initiator concentration, the propagation speed is different in each domain. We study fronts propagating in two parallel strips in which the incident angle is 90°. Our data fit Snell's law $v_r/v_i=\sin\theta_r/\sin\theta_i$, where v_r is the refracted velocity, v_i is the incident velocity, θ_r is the angle of refraction, and θ_i is the incident angle. Further, we study circular fronts propagating radially from an initiation point in a high-velocity region into a low-velocity region (and vice versa). We demonstrate the close resemblance between the numerically simulated and experimentally observed thermal reaction fronts. By measuring the normal velocity and the angle of refraction of both simulated and experimental fronts, we establish that Snell's law holds for thermal frontal polymerization in our experimental system. Finally we discuss the regimes in which Snell's law may not be valid. © *2007 American Institute of Physics*. [DOI: 10.1063/1.2784386]

Refraction of light waves is governed by Snell's law $\sin\theta_i/\sin\theta_r=n$, where n is the relative index of refraction, θ_i is the angle of the incident wave and θ_r is the angle of the refracted wave. More generally, Snell's law describes the behavior of any steadily propagating front when it crosses the boundary between two media with unequal constant velocities of propagation. We study chemical fronts sustained by an exothermic polymerization reaction. We demonstrate both experimentally and numerically that refraction of polymerization fronts can be accurately described by Snell's law.

I. INTRODUCTION

Snell's law establishes the relationship between the angles of incidence and refraction for a wave passing through the boundary between two media with different refractive indices

$$\frac{n_i}{n_r}=\frac{\sin\theta_r}{\sin\theta_i}. \tag{1}$$

Here, n_i and n_r are the refractive indices, θ_r is the angle of refraction, and θ_i is the incident angle.

Instead of using refractive indices in this relationship, the front velocity can be used instead because

$$\frac{n_r}{n_i}\propto\frac{v_i}{v_r}. \tag{2}$$

The relationship (1) takes the form

$$\frac{v_r}{v_i}=\frac{\sin\theta_r}{\sin\theta_i}, \tag{3}$$

where v_r is the refracted velocity and v_i is the incident velocity.

Although it was originally formulated for electromagnetic waves, generally Snell's law is valid for refraction of sharp fronts that can be described by an eikonal equation within a geometric diffraction theory. For singularly perturbed reaction-diffusion systems with slow diffusion, the applicability of geometric theory to propagation of reaction waves has been established. Using formal asymptotic arguments, Keener showed that sharp reaction fronts are described by a generalized eikonal equation

$$V_n=U+D\kappa,$$

where V_n is the normal velocity of the front, κ is the curvature of the front, U is the speed of the planar front in a uniform medium, and D is related to the diffusion coefficient.[1] When D is small, the second term can be neglected (as long as the curvature of the front is not too large) leading to the standard eikonal equation.

Note that, if two fronts meet at an angle on the boundary between two media, the curvature term goes to infinity at the point of the junction. Thus, the curvature term "smooths out" the transition between two parts of the front with the transition becoming sharper as D tends to zero.

Experimentally, the applicability of Snell's law to chemical waves in the Belousov-Zhabotinsky system was demonstrated by Zhabotinsky and Epstein[2] as well as other groups.[3–5] Sainhas and Dilão simulated refraction and reflec-

tion in reaction-diffusion systems.[5] Fialkowski *et al.* demonstrated refraction and reflection with Liesegang rings.[6] Steinbock *et al.* studied BZ waves propagating along adjacent strips in which the fronts had different velocities.[7]

Generally, however, the angle between refracted and incident fronts in reaction-diffusion systems does not have to obey Snell's law. Indeed, Mornev has recently shown that refraction of chemical waves might follow a tangent rule when mass diffusion is sufficiently fast.[8]

There have been several reports that thermal fronts, generated by rapid heating, follow Snell's law.[9] However, to our knowledge, no one has considered refraction of reaction-diffusion fronts based on an exothermic reaction. As a model system for studying thermal fronts, we have chosen frontal polymerization.

Thermal frontal polymerization begins when a heat source is brought in contact with a reactive monomer system. The area of contact has a faster polymerization rate, and the energy from the exothermic polymerization diffuses into the adjacent region, raising the temperature and increasing the reaction rate in that location. The result is a localized reaction zone that propagates down the reaction vessel as a thermal front.[10,11]

II. SELECTION OF SYSTEM

Frontal polymerization can be performed with many different types of polymerization systems (see http://www.pojman.com/FP_Bibliography.html for a comprehensive bibliography of frontal polymerization). We chose to use free-radical polymerization fronts[11] because velocities of such fronts can be easily controlled by changing the concentration of the initiator.[12]

The experiments used a mixture of the monomer trimethylolpropane triacrylate (TMPTA-N), the initiator Luperox 231, and a kaolin clay filler Polygloss 90. The filler constituted 47% of the total weight in each trial, giving the mixture the consistency of putty and eliminating the effects of buoyancy-driven convection in the medium.[13] (We did not attempt to control convection in the air caused by the heat from the reaction.) The clay did not quench the fronts because acrylates are highly reactive, and multifunctional acrylates like TMPTA-N support fronts with velocities at least an order of magnitude greater than monofunctional acrylates.[12,14] We minimized bubbling by using 1,1-bis(tert-butylperoxy)-3.3.5-trimethylcyclohexane (Luperox® 231P75), which releases less gas per initiating radical than other peroxide initiators.[15]

We spread the putty uniformly on a wooden substrate and constrained it between wooden strips to provide thermal insulation beneath the putty and at the sides. By performing the experiments under adiabatic conditions we eliminated the effects of heat losses on the front shape and allowed for simpler modeling and simulation. By performing the experiments horizontally, we ensured that possible convective losses at the front did not influence the polymerization of the rest of the putty.

In order to enhance detection of the front, we added a small amount of the *p*H-sensitive dye bromophenol blue dissolved in dimethyl sulfoxide (DMSO).[16] The free radicals in the reaction bleached the dye, making the demarcation between reacted and unreacted regions evident.

III. EXPERIMENT

Trimethylolpropane triacrylate (TMPTA-N) was obtained from CYTEC, Surface Specialties. 1,1-bis(tert-butylperoxy)-3.3.5-trimethylcyclohexane (Luperox® 231P75) was obtained from Atofina and Polygloss 90 from Huber materials. All reagents were used as-received.

Two types of experiments were performed. In the first one, two strips of putty 17 cm × 2.0 cm × 0.5 cm were prepared, each with a different concentration of initiator. The strips were placed in contact such that 6 cm of each strip was not in contact with the other strip. A front in the strip containing the higher concentration of initiator was ignited with a soldering iron. The fronts achieved their steady-state velocity in about 3 cm. The velocity in each strip was calculated from a plot of the position versus time for each individual region that did not overlap with the other strip. Front velocities ranged from 0.5 cm min^{-1} for 1% of the initiator to 9 cm min^{-1} for 5%, and the front temperatures were about 200 °C. The experiments were recorded using an iSight camera and iMovie software.

In the second type of experiment, two larger domains with different initiator concentration were created. A circular propagating front was initiated with a soldering iron in one of the domains [see Figs. 4(a) and 6(a) below].

IV. NUMERICAL METHOD

We conducted numerical experiments with a one-step reaction model in the absence of material diffusion

$$M_t = -K(T)M, \tag{4}$$

$$T_t = \kappa \Delta T + qK(T)M, \tag{5}$$

where M is the monomer concentration, T is the temperature, κ is a coefficient of heat diffusion, and q is the heat release. The reaction term involves

$$K(T) = k\sqrt{I}e^{-E/RT}, \tag{6}$$

where I is the constant initiator concentration, E is the effective activation energy, and R is the universal gas constant. The system of equations was solved numerically in two spatial dimensions using an Alternating Directions Implicit (ADI) finite difference method with semi-implicit time integration.[17] The physical model has no-flow homogeneous Neumann boundary conditions on all sides of the domain.

For the initial conditions we chose piecewise-constant functions

$$M = \begin{cases} 0, & x \in \omega, \\ M_0, & x \in \Omega - \omega, \end{cases} \qquad T = \begin{cases} T_b, & x \in \omega, \\ T_0, & x \in \Omega - \omega. \end{cases}$$

Here M_0, T_0 are initial monomer concentration and initial temperature, respectively, T_b is the temperature of the reaction products, Ω is the domain of the simulation, and $\omega \subset \Omega$ is the region where the reaction has already occurred by the time $t=0$. At each time step t_n, the location of the reaction

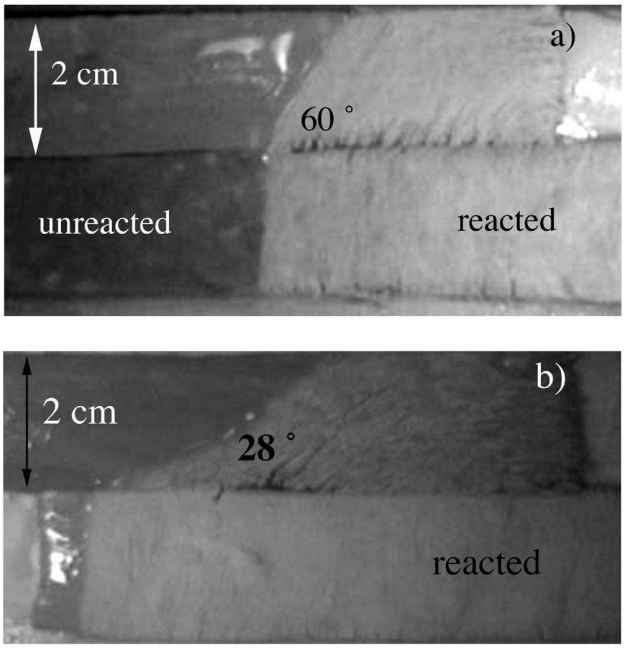

FIG. 1. Refraction of polymerization fronts between two parallel strips propagating from the right to the left. (a) Fronts with 2% (top) and 3% (bottom) initiator. (b) Fronts with 1% (top) and 3% (bottom) initiator.

front was defined as the level set $M(x,t_n)=\frac{1}{2}$, i.e. where the concentration of the monomer drops below 50% of the initial value. The reference velocity of a front, steadily propagating in a uniform mixture, was calculated in numerical simulations of the governing system of equations in one spatial dimension. Then the average velocity of the steadily propagating front is

$$v = a\frac{\Delta x}{\Delta t}, \tag{7}$$

where Δx is the distance between grid points, Δt is the size of the time step, and a is the number of grid intervals traveled through by the front in Δt seconds. Note that it may take multiple, say m, time steps for the front to travel through one grid interval. In that case, we have $a=1/m$.

We used a uniform grid refinement technique, which clearly indicated numerical convergence and demonstrated that all sharp features are resolved and grid independent. We used parameter values $q=33.24$ K l/mol, $\kappa=0.0014$ cm^2 s^{-1}, $k=1$ s^{-1}, $T_b=500$ K. The dimensions of the spatial domain in our computations vary depending on which experiment is simulated.

V. RESULTS

A. Experiments with strips

Figure 1 presents images of incident and refracted fronts traveling to the left in strips that support different traveling-wave velocities. In Fig. 1(a), the velocities of the fronts in the individual strips are closer to each other than those in the two strips in Fig. 1(b). Thus, the refracted angle is larger in Fig. 1(a) than in Fig. 1(b).

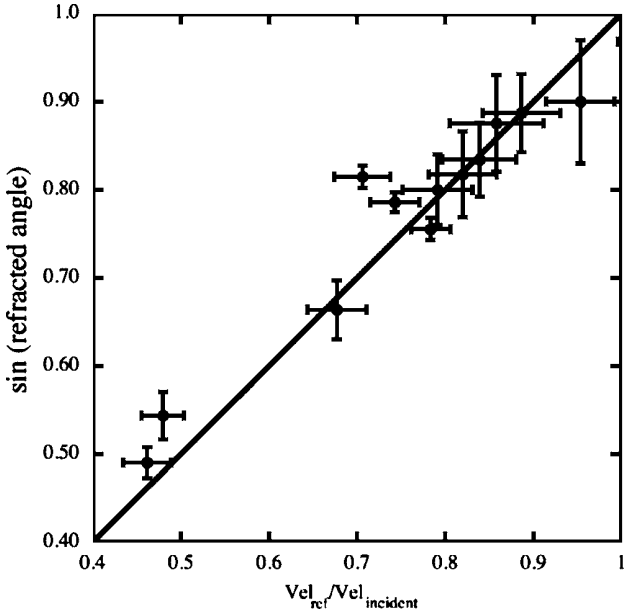

FIG. 2. Plot of the sine of the refracted angle vs the ratio of the refracted and incident velocities for the type of experiments shown in Fig. 1.

In the strip experiments the faster front had an incident angle of approximately 90°. Any discrepancies with a 90° angle can be attributed to several factors including slight variations in the composition, minor nonuniformity in the thickness of the sample, heat losses, and thermal stress. (Note that the numerically determined front, see Fig. 3 below, settles into a configuration in which the faster portion propagates steadily at a 90° angle to the longitudinal axis.) We assumed that the sine of the incident angle in our experiments was equal to 1. Figure 2 shows a plot of the sine of the refracted angle versus the ratio of the velocity of the refracted front to the velocity of the incident front for experiments shown in Fig. 1, as well as for similar experiments. The agreement between experiment and theory is very good. We were not able to test the agreement for velocity ratios smaller than about 1/2. To do so would require much longer samples to allow the fronts to reach steady-state propagation. Figure 3 presents a simulation of the type of experiment in Fig. 1. The simulation accurately reproduces the behavior seen experimentally (Fig. 1) and is also consistent with Snell's law.

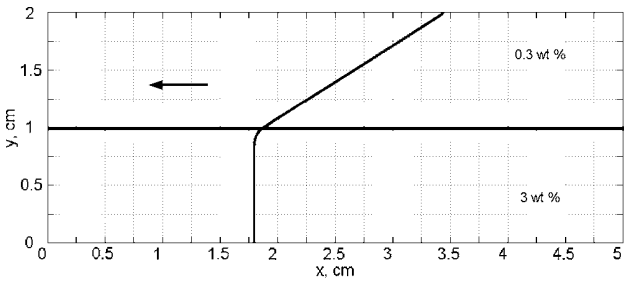

FIG. 3. Numerical simulation of refraction. The angle of refraction is 30° and vel$_{ref}$/vel$_i$=0.154/0.304=0.505.

B. Circular experiments

Inspired by the experiments of Hwang and Halpin-Healy[3] and Fialkowski *et al.*[6] we studied fronts that were ignited near the boundary between regions of different velocities. These experiments allow us to test indirectly the validity of Snell's law: We compare the front shape to analytical predictions derived from the assumption that Snell's law holds on the boundary between the two media. Figures 4 and 6 show the experimental configurations (a) and the results of simulations (b). The results are consistent in each figure.

We applied the analysis of Hwang and Halpin-Healy[3] for the front shape after refraction in the regime that corresponds to Fig. 4(a); Eqs. (8) and (9) provide the coordinates for the refracted wave front relative to the point of initiation when the front propagates from a high-velocity region to a low-velocity region as in Fig. 4. The time-dependent radius of the incident reaction front is given by R. The front was initiated at the perpendicular distance $d=1$ cm from the boundary between the regions (Fig. 4),

$$x = \frac{[d(n^2-1)\tan\alpha + R\sin\alpha]}{n^2}, \tag{8}$$

$$y = \frac{[(R - d\sec\alpha)\sqrt{n^2-\sin^2\alpha}]}{n^2}, \quad 0 < \alpha < \cos^{-1}(d/R). \tag{9}$$

The maximum vertical distance between the refracted front and the boundary between the regions is denoted by *dref*. The refractive index n was calculated by $n=(R-d)/dref$ The fronts calculated from Eqs. (8) and (9) are compared to experimental fronts in Fig. 5. The theory agrees very well with the experimental results.

We also performed the experiment and numerical simulation when the polymerization front propagated from the region with slower velocity to the region with the faster velocity (Fig. 6) with numerical predictions matching the experimental results.

Note that, although we did not compare experimental observations with theoretical predictions from Eqs. (8) and (9) in this case, the analysis of Hwang and Halpin-Healy still applies for short times after the incident front crosses the boundary from the region with a slower velocity [bottom region in Fig. 6(a)] to the region with faster velocity [top region in Fig. 6(a)]. When $t=d/v\sqrt{1-n^2}$, the front in the region with faster velocity is orthogonal to the boundary between the regions and it begins to propagate along that boundary. The faster front is then refracted toward the region with slower velocity. Thus the refracted front becomes an incident front and vice versa as can be seen from the "mushroom" shape of the fronts in Fig. 6.

The final experimental setup consisted of three parallel strips of putty: two identical outer strips with 6% initiator and a significantly narrower inner strip with 5% initiator (Fig. 7). The front propagation speed in the regions with 5% of initiator is about 10% faster than in the regions with 6% of initiator. (The front velocity is a maximum with 5% initiator

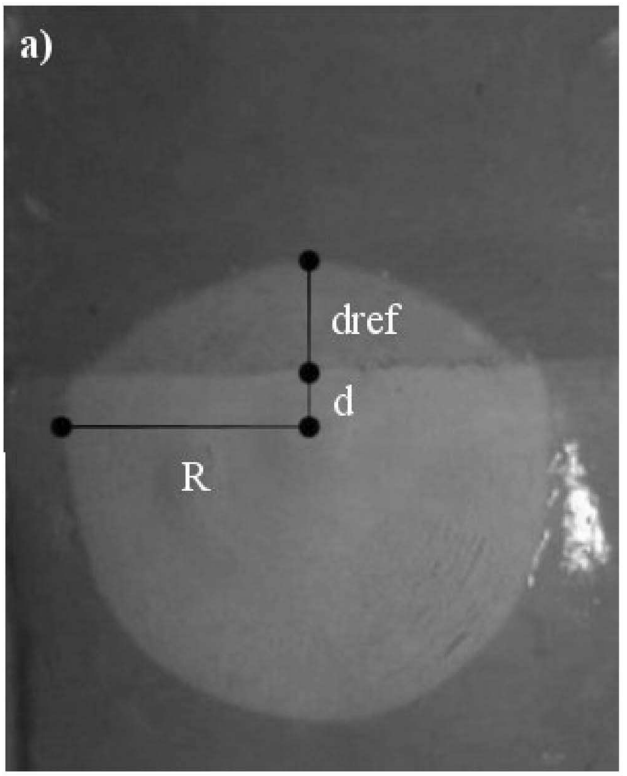

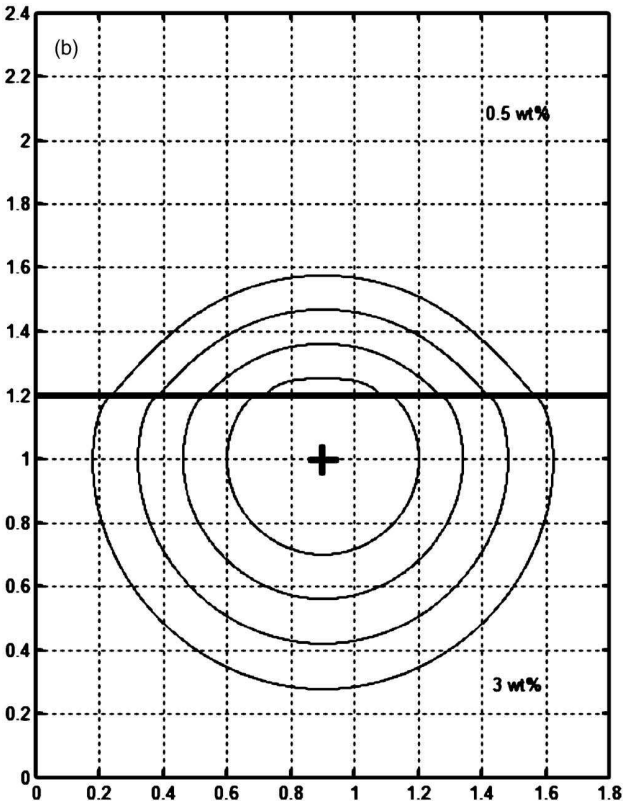

FIG. 4. (a) A refracted front is shown propagating from a "fast" region (bottom) containing 3% initiator into a "slow" region (top) with 1% initiator. The horizontal width of each domain is 15 cm and the radius of the front in the "fast" region is $R=3.5$ cm. (b) Numerical simulation of a front propagating from a "fast" region (bottom) containing a 3% initiator to a "slow" region (top) with 0.5% initiator.

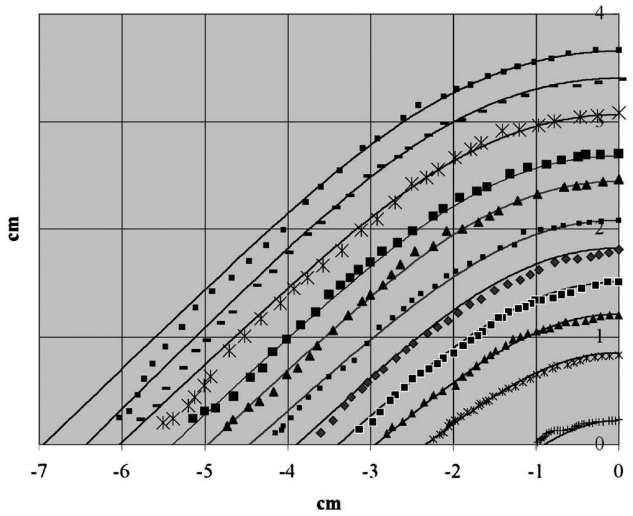

FIG. 5. Positions of the front at various times between $t=10$ s and $t=48$ s for the refracted wave front in the experiment shown in Fig. 4(a) (discrete points), together with the analogous front positions calculated from Eqs. (8) and (9) (solid lines).

and decreases with higher initiator concentration.) The three-strip configuration mimics the setup of Steinbock *et al.* for BZ waves.[7]

We found that the fronts in the three-strip system remain essentially straight within each strip and continuous between the strips (Fig. 7). This indicates that Snell's law holds on both interstrip boundaries present in the system. The main difference between our experiment and a similar experiment by Steinbock *et al.*[7] is that the front remains straight in the middle strip in our setup. We attribute the difference to the fact that, although the middle strip is narrow in our experiments, it is an order of magnitude wider than that in Steinbock *et al.* Notice that the front is slightly curved on the boundary between two strips (Fig. 7). When the middle strip is sufficiently narrow, the curved parts of the front combine resulting in the curved profile observed by Steinbock *et al.*

VI. DISCUSSION

For all studied concentration differences of the initiator mixtures, most data points from the two-strip experiments fall on the line predicted by Snell's law as shown in Fig. 2. Further, error bars demonstrate that experimental data points that do not fall precisely on the theoretical curve are, however, within experimental error of their predicted values. Some bubbling under the surface of the higher concentration of peroxide initiator occurred and could have slowed the front and distorted the angle, thereby leading to a discrepancy with Snell's law. Additional causes for variations from predicted angles of refraction are expansion and contraction of the system during polymerization and stress-induced cracking. However, the graph of the sine of the refracted angle versus the ratio of the refracted and incident velocities demonstrates the good agreement between the theoretical and experimental data. It allows us to conclude that the strip experiment obeys Snell's law of refraction.

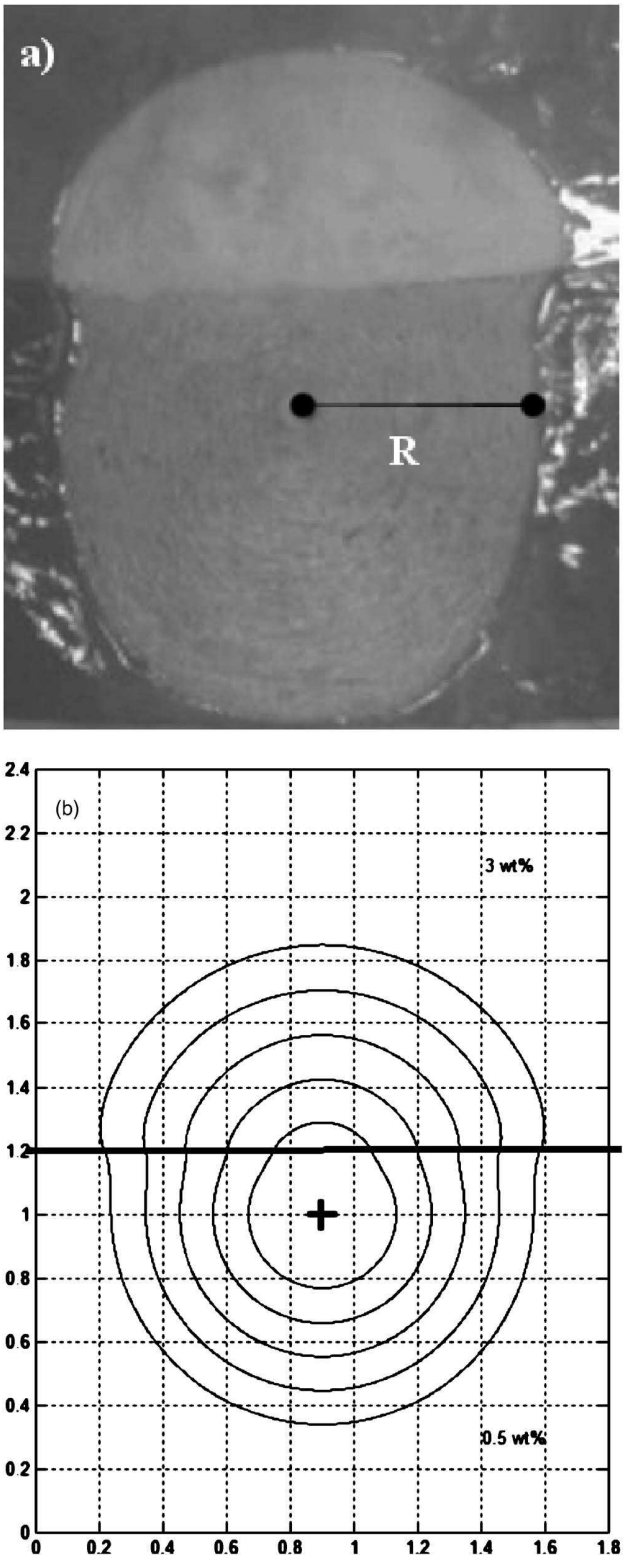

FIG. 6. (a) A refracted front is shown propagating from a "slow" region (bottom) containing a 3% initiator into a "fast" region (top) with 1% initiator. The horizontal width of each domain is 15 cm and the radius of the front in the "fast" region is $R=3.5$ cm. (b) Numerical simulation of a front propagating from a slow to a fast region.

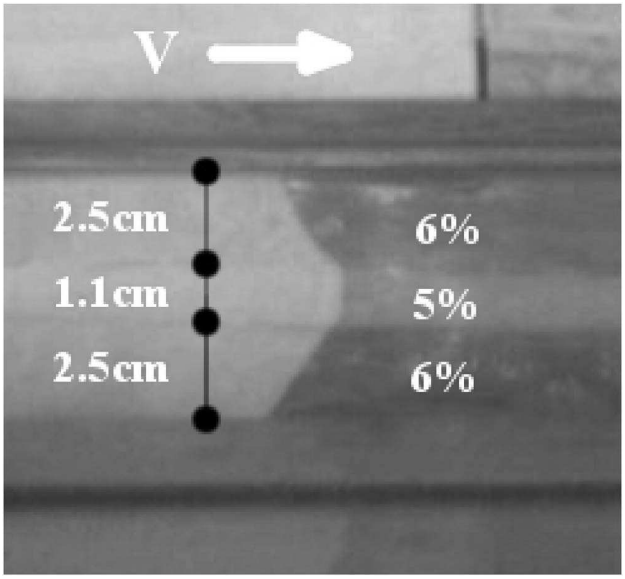

FIG. 7. A refracted front is shown propagating through three parallel strips with 6%-5%-6% initiator concentration.

The circular fronts demonstrate the same result as for the parallel strips. The graph in Fig. 5 shows the good agreement between the experimental refracted fronts initiated in a region with a faster velocity of propagation and those predicted by Eqs. (8) and (9) of Hwang and Halpin-Healy.[3] Initially, the theoretical and experimental fronts differ, but the discrepancy disappears about 15 s from initiation. Thereafter, the predicted and experimental curves agree closely. Although they were not compared here, we expect that the experimental front profiles shown in Fig. 6(a) match with those predicted by the same analytical formula as well.

Numerical simulations for refracted fronts initiated in regions with both fast and slow speeds of propagation [Figs. 4(b) and 6(b)] qualitatively match the experimental results [Figs. 4(a) and 6(a), respectively]. Thus, the relatively simple, one-step reaction-diffusion system [Eqs. (4) and (5)] correctly captures the experimentally observed sharp front dynamics even though it is not intended to model the evolution of concentration and temperature precisely.

Note that, even though the fronts are essentially flat in the strip studies and obey Snell's law, the incident and refracted fronts pass through a narrow transition zone near the boundary between the two media in which the reaction front appears curved (see, e.g., Figs. 1 and 3). As such this configuration is different from the one used in the standard geometric proof of Snell's law, which shows two straight rays emanating from a point. However, the same geometric proof still applies to our configuration as long as the front remains flat away from the transition zone.

As we discussed in the Introduction, the evolution of sharp reaction fronts propagating in systems with slow diffusion can be described by a generalized eikonal equation with an additional curvature term that vanishes as the (heat) diffusion coefficient tends to zero. This term has an effect of curving the front in a transition zone between the incident and the refracted fronts.

Said differently, for frontal reactions discussed thus far, the heat exchange between the "fast" and the "slow" strips is significantly slower than the speed of a sharp front (which is established through a balance between the rates of reaction and diffusion). Then the propagation of the "fast" front is not affected by the presence of the "slow" strip away from the boundary between the regions and vice versa. The slow heat exchange between the regions leads only to slight curving of the front near the boundary between the two media, while the refraction is still governed by Snell's law.

If, on the other hand, the diffusion was stronger, then the front in the "fast" region would be significantly affected by the heat exchange with the "slow" region and vice versa; the angle between the reaction fronts in two regions would be dictated by the continuity of the heat flux through the boundary between the regions,[8] and the fronts would deviate from the linear shape farther from their junction at the boundary. The two fronts would no longer appear flat.

To see whether we could observe curved fronts in our experimental system, we performed a three-strip experiment with the narrowest middle strip that we could mold. Even in this case, the front remains essentially linear in each region (see Fig. 7). Hence the angles between segments are determined by Snell's law.

VII. CONCLUSIONS

In this paper, a system with reaction-diffusion fronts based on an exothermic reaction was studied using two different types of experiments. In the first experiment, either two or three strips with different concentrations of the peroxide initiator concentration were placed side-by-side in contact with each other. Decreasing the initiator concentration difference between the domains decreased the angle of refraction as the ratio of incident and refracted velocities decreased. Independent of variation of the initiator concentration between the domains, the sine of the incident angle was approximately equal to 1. We verified that the reaction front propagation in these systems follows Snell's law of refraction.

In the second type of experiment, the validity of Snell's law for radially propagating fronts was established by comparing experimental fronts to those predicted by an analytical formula of Hwang and Halpin-Healy.[3] Experimental observations were also supported by numerical simulations of refracted and incident fronts within one-step free radical polymerization model.

Thus, we demonstrate for the first time that Snell's law of refraction holds for reaction-diffusion fronts based on an exothermic reaction.

[1]J. P. Keener, SIAM J. Appl. Math. **46**, 1039 (1986).
[2]A. M. Zhabotinsky, M. D. Eager, and I. R. Epstein, Phys. Rev. Lett. **71**, 1526 (1993).
[3]S.-C. Hwang and T. Halpin-Healy, Phys. Rev. E **54**, 3009 (1996).
[4]A. Lazar, H. D. Forsterling, A. Volford *et al.*, J. Chem. Soc., Faraday Trans. **92**, 2903 (1996).
[5]J. Sainhas and R. Dilão, Phys. Rev. Lett. **80**, 5216 (1998).
[6]M. Fialkowski, A. Bitner, and B. A. Grzybowski, Phys. Rev. Lett. **94**, 018303 (2005).
[7]O. Steinbock, V. S. Zykov, and S. C. Müller, Phys. Rev. E **48**, 3295 (1993).

[8]O. A. Mornev, JETP Lett. **80**, 721 (2004).
[9]M. Bertolotti, G. L. Liakhou, R. L. Voti *et al.*, J. Appl. Phys. **85**, 3540 (1999); M. L. Shendeleva, Phys. Rev. B **65**, 134209 (2002); A. Mandelis, L. Nicolaides, and Y. Chen, Phys. Rev. Lett. **87**, 020801 (2001).
[10]N. M. Chechilo, R. J. Khvilivitskii, and N. S. Enikolopyan, Dokl. Akad. Nauk SSSR **204**, 1180 (1972); S. P. Davtyan, P. V. Zhirkov, and S. A. Vol'fson, Russ. Chem. Rev. **53**, 150 (1984); A. M. Khan and J. A. Pojman, Trends Polym. Sci. **4**, 253 (1996).
[11]J. A. Pojman, V. M. Ilyashenko, and A. M. Khan, J. Chem. Soc., Faraday Trans. **92**, 2825 (1996).
[12]J. A. Pojman, J. Willis, D. Fortenberry *et al.*, J. Polym. Sci., Part A: Polym. Chem. **33**, 643 (1995); P. M. Goldfeder, V. A. Volpert, V. M. Ilyashenko *et al.*, J. Phys. Chem. B **101**, 3474 (1997).
[13]G. Bowden, M. Garbey, V. M. Ilyashenko *et al.*, J. Phys. Chem. B **101**, 678 (1997).
[14]C. Nason, T. Roper, C. Hoyle *et al.*, Macromolecules **38**, 5506 (2005).
[15]B. Binici, D. I. Fortenberry, K. C. Leard *et al.*, J. Polym. Sci., Part A: Polym. Chem. **44**, 1387 (2006).
[16]J. Masere and J. A. Pojman, J. Chem. Soc., Faraday Trans. **94**, 919 (1998).
[17]J. Douglas, J. Soc. Ind. Appl. Math. **3**, 42 (1955).